PLOS ONE

RESEARCH ARTICLE

Retinal Neuroprotective Effects of Flibanserin, an FDA-Approved Dual Serotonin Receptor Agonist-Antagonist

Aaron S. Coyner[1], Renee C. Ryals[1], Cristy A. Ku[1], Cody M. Fischer[1], Rachel C. Patel[1], Shreya Datta[1], Paul Yang[1], Yuquan Wen[2], René Hen[3], Mark E. Pennesi[1]*

1 Casey Eye Institute, Oregon Health & Science University, Portland, Oregon, United States of America, **2** Baylor University Medical Center, Dallas, Texas, United States of America, **3** New York State Psychiatric Institute, Columbia University, New York, New York, United States of America

* pennesim@ohsu.edu

Citation: Coyner AS, Ryals RC, Ku CA, Fischer CM, Patel RC, Datta S, et al. (2016) Retinal Neuroprotective Effects of Flibanserin, an FDA-Approved Dual Serotonin Receptor Agonist-Antagonist. PLoS ONE 11(7): e0159776. doi:10.1371/journal.pone.0159776

Editor: Thomas Langmann, University of Cologne, GERMANY

Received: February 27, 2016

Accepted: June 7, 2016

Published: July 22, 2016

Data Availability Statement: All relevant data are within the paper and its Supporting Information files.

Funding: This work was supported by K08 Career Development Award K08 EY021186 (MEP); Alcon Young Investigator Award (MEP); Foundation Fighting Blindness Enhanced Research and Clinical Training Award CD-NMT-0914-0659-OHSU (MEP); Career Development Award from Research to Prevent Blindness (MEP); also supported by unrestricted departmental funding from Research to Prevent Blindness (New York, NY) and by grant P30 EY010572 from the National Institutes of Health

Abstract

Purpose

To assess the neuroprotective effects of flibanserin (formerly BIMT-17), a dual 5-HT_{1A} agonist and 5-HT_{2A} antagonist, in a light-induced retinopathy model.

Methods

Albino BALB/c mice were injected intraperitoneally with either vehicle or increasing doses of flibanserin ranging from 0.75 to 15 mg/kg flibanserin. To assess 5-HT_{1A}-mediated effects, BALB/c mice were injected with 10 mg/kg WAY 100635, a 5-HT_{1A} antagonist, prior to 6 mg/kg flibanserin and 5-HT_{1A} knockout mice were injected with 6 mg/kg flibanserin. Injections were administered once immediately prior to light exposure or over the course of five days. Light exposure lasted for one hour at an intensity of 10,000 lux. Retinal structure was assessed using spectral domain optical coherence tomography and retinal function was assessed using electroretinography. To investigate the mechanisms of flibanserin-mediated neuroprotection, gene expression, measured by RT-qPCR, was assessed following five days of daily 15 mg/kg flibanserin injections.

Results

A five-day treatment regimen of 3 to 15 mg/kg of flibanserin significantly preserved outer retinal structure and function in a dose-dependent manner. Additionally, a single-day treatment regimen of 6 to 15 mg/kg of flibanserin still provided significant protection. The action of flibanserin was hindered by the 5-HT_{1A} antagonist, WAY 100635, and was not effective in 5-HT_{1A} knockout mice. *Creb*, *c-Jun*, *c-Fos*, *Bcl-2*, *Cast1*, *Nqo1*, *Sod1*, and *Cat* were significantly increased in flibanserin-injected mice versus vehicle-injected mice.

(Bethesda, MD). The funders had no role in study design, data collection and analysis, decision to publish, or preparation of the manuscript.

Competing Interests: MEP is a consultant for Sucampo. This does not alter the authors' adherence to PLOS ONE policies on sharing data and materials.

Conclusions

Intraperitoneal delivery of flibanserin in a light-induced retinopathy mouse model provides retinal neuroprotection. Mechanistic data suggests that this effect is mediated through 5-HT_{1A} receptors and that flibanserin augments the expression of genes capable of reducing mitochondrial dysfunction and oxidative stress. Since flibanserin is already FDA-approved for other indications, the potential to repurpose this drug for treating retinal degenerations merits further investigation.

Introduction

Inherited retinal dystrophies (IRDs), such as retinitis pigmentosa, are clinically and genetically diverse, and account for approximately 5% of the vision loss in the Western world. [1–3] There are no effective treatments for most of these disorders, but gene therapy shows promise for a small subset of IRDs. [4–8] However, with almost 180 genes and thousands of distinct mutations, developing gene replacement strategies for all IRD patients will be a long and difficult endeavor. [2] The development of gene-independent therapies is therefore essential in preserving retinal morphology and function until suitable gene therapies can be developed. Additionally, synergistic rescue may be achieved with neuroprotective agents in combination with gene or cell-based therapies.

The neurotransmitter, serotonin (5-hydroxytryptamine or 5-HT), has been shown to modulate retinal processing, although the full extent of the role of serotonin in the retina remains unclear. [9–20] 5-HT receptors have been sub-divided into seven major classes (5-HT_{1-7}) based on structural, functional and pharmacological criteria, with distinct molecular properties further dividing these classes into over 17 different subtypes. [14, 21] Chen et al. demonstrated evidence for gene expression of 5-HT receptors in the mammalian retina using quantitative transcriptome analysis. [22] Localization studies expressing eGFP under the endogenous 5-HT receptor promoter suggest the presence of 5-HT_{2A} and 5-HT_{3A} receptors in bipolar cells,[23, 24] and 5-HT_{2A} in photoreceptor terminals. [25] Despite evidence of serotonin and 5-HT receptors in the mammalian retina, their likely low expression in the retina has hindered exact localization and evaluation of function. [22]

Recent studies conducted by our lab and others suggest that certain serotonin receptor agonists and antagonists provide neuroprotection against light-induced retinopathy. [15–20, 26] 5-HT_{1A} receptor agonists, such as 8-OH-DPAT and AL-8309B, provided anti-oxidant protection against light-damage in albino rats and in a genetic mouse model for AMD. [15–17] 5-HT_{2A} receptor antagonists, ketanserin and sarpogrelate, protected against light-induced retinopathy in albino Balb/c mice and in the Stargardt *Abca4*$^{-/-}$*Rdh8*$^{-/-}$ mouse model. [20, 26] In addition, simultaneous treatment with a 5-HT_{1A} agonist and a 5-HT_{2A} antagonist has shown an additive neuroprotective effect. [20, 22, 27] Altogether, these reports suggest that 5-HT_{1A} receptor agonists and 5-HT_{2A} receptor antagonists can elicit neuroprotective effects in the retina and warrant their continued investigation as a therapeutic class in treatment of retinal degeneration.

Flibanserin, marketed as Addyi™ (Sprout Pharmaceuticals), was recently approved by the Food and Drug Administration (FDA) for the treatment of hypoactive sexual desire disorder (HSDD). [28–33] Seven phase III clinical trials demonstrated that a daily 100 mg dose of flibanserin was safe and resulted in an improvement of HSDD-related symptoms in pre-menopausal women. [30–33] In CHO cells, flibanserin has a high affinity for serotonergic 5-HT_{1A}

and 5-HT_{2A}, as well as dopaminergic D_4 receptors, although D_4 receptor binding has yet to be verified in human brain tissue. [34–39]

The determination of retinal protection and cell survival mechanisms conferred by neuroprotective agents, such as flibanserin, is aided by evaluation in models with widely-described cell death mechanisms. The relatively synchronous and rapid progression of apoptosis in light-induced retinopathy has provided many insights into the mechanisms of cell death. [40] Therefore, to evaluate the neuroprotective potential of flibanserin and its mechanism of action, we tested it in the well-established light-induced retinopathy model. [20, 41–45]

Methods

Animals

All experiments and animal handling procedures were approved by and performed in compliance with the policies of the Institutional Animal Care and Use Committee at Oregon Health & Science University (IACUC Protocol Number IS03147) and adhered to the ARVO Statement for the Use of Animals in Ophthalmic and Vision Research. Albino BALB/cJ mice were purchased from The Jackson Laboratory (Bar Harbor, ME). 5-$HT_{1A}^{-/-}$ mice (5-HT_{1A} knockout mice) were generously provided by Dr. René Hen (Columbia University, New York, NY). [46] 5-$HT_{1A}^{-/-}$ mice were originally on a pure 129/Sv background, but backcrossed with albino BALB/c mice for nine generations (F9) before being used in experiments. Genotypes were confirmed using PCR. Mice utilized in these studies were males between two and three months old. Mice were housed in a 12-hour alternating light/dark cycle room. The light cycle (~15 lux) occurred from 9:00 PM to 9:00 AM, and dark cycle from 9:00 AM to 9:00 PM. Following data acquisition, all mice were euthanized via gradual CO_2 inhalation and cervical dislocation.

PCR Genotyping

PCR analysis was performed using Quick-load Taq (Taq 2x Master Mix, New England Biolabs, Ipswich, MA) and the following primer sequences (Integrated DNA Technologies, San Diego, CA): 5-HT_{1A} promoter (forward): 5′ -CAG TCT CTA GAT CCC CTC CCT-3′ ; 5-HT_{1A} coding sequence (reverse): 5′ -GGG CGT CCT CTT GTT CAC GTA-3′ ; and tTA insert (reverse): 5′ -AAG GGC AAA AGT GAG TAT GGT-3′ . A 25 μL PCR reaction was performed in a Veriti thermal cycler (Applied Biosystems, Coster City, CA). Each PCR reaction consisted of 12.5 μL Quick-load Taq, 1 μL of primer mix (1 μL of 200 μg/μL 5-HT_{1A} promoter, 0.5 μL of 200 μg/μL 5-HT_{1A} coding sequence, 0.5 μL of 200 μg/μL tTA insert, and 18 μL distilled H_2O), 1 μL genomic DNA, and 10.5 μL distilled H_2O. PCR cycle was as follows: initial denaturation for 1 minute at 95°C, then 30 cycles of 95°C for 45 s, 50°C for 30 s, 72°C for 60 s, and a final extension at 72°C for 60 s. No-template DNA controls, wildtype, and 5-HT_{1A} heterozygote and homozygote controls were utilized with each PCR genotyping experiment. PCR products were analyzed via gel electrophoresis using a 1.5% agarose gel ran at 90 mV for 50 minutes. Bands were visualized using EZ-Vision (EZ-Vision Three DNA Dye as Loading Buffer 6X, Amresco, Solon, OH) and a UV transilluminator (GelDoc-It, UVP, Upland, CA). The WT and KO alleles were identified as 600 bp and 300 bp PCR products, respectively.

Drug Preparation

Flibanserin (Sigma-Aldrich, St. Louis, MO) was dissolved in Kollisolv PEG E 400 (PEG 400) (Sigma-Aldrich, St. Louis, MO), warmed to 60°C and diluted to 35% (v/v) in 0.9% saline (Hospira, Inc., Lake Forest, IL). The vehicle was 35% (v/v) PEG 400 in 0.9% saline. WAY 100635 was dissolved in 0.9% saline. The vehicle for this experiment was 0.9% saline.

Five-Day Drug Time Course

Two hours into the 12-hour dark cycle, mice were injected intraperitoneally (10 mL/kg) under dim red light. Mice were dosed with vehicle, 0.75, 1.5, 3.0, 6.0, 9.0 or 15 mg/kg flibanserin 48 hours, 24 hours and immediately prior to a one-hour bright light exposure, and 24 and 48 hours after light exposure. Naïve mice were not injected or exposed to bright light.

One-Day Drug Time Course

Two hours into the 12-hour dark cycle, mice were injected intraperitoneally (10 mL/kg) under dim red light. A single dose of vehicle, 3, 6, 9 or 15 mg/kg of flibanserin was administered immediately before a one-hour bright light exposure in order to evaluate a shortened one-day treatment regimen. To assess 5-HT_{1A}-mediated effects, 10 mg/kg WAY 100635, a selective 5-HT_{1A} antagonist (K_i = 2),[47] was administered to mice 30 minutes prior to 6 mg/kg flibanserin. Additionally, 5-$HT_{1A}^{-/-}$ mice were also administered 6 mg/kg flibanserin immediately prior to bright light exposure. Because WAY 100635 is also a potent D_4 agonist (K_i = 16),[47] 10 mg/kg WAY 100635 was injected alone prior to bright light exposure in order to assess whether a D_4 agonist, delivered at a concentration similar to that of 15 mg/kg flibanserin, could provide any neuroprotective effects against light-induced retinopathy. Naïve mice were not injected or exposed to bright light.

Light-Induced Retinopathy

Four compact fluorescent lamps (42 watts, 6500K) were installed in a custom-built light box producing 10,000 lux of uniform light, and capable of holding 16 mice. [20] Two hours into the 12-hour dark cycle, mice were placed into the light box and exposed to bright light for one hour. Temperature and humidity were regulated using a portable air conditioning unit. Mice were monitored throughout light exposure and were given access to water. Vehicle-injected control mice were used in each experiment to ensure the occurrence of light-induced retinopathy. [20]

In Vivo OCT Imaging

Retinas were imaged as previously reported. [20, 48] Seven days following bright light exposure, mice were sedated using 1.5% isoflurane delivered via a nose cone, corneas were anesthetized with 0.5% proparacaine, and pupils were dilated using a combination of 1% tropicamide and 2.5% phenylephrine. Artificial tears were used to maintain corneal clarity. Mice were seated in a Bioptigen AIM-RAS holder and spectral domain optical coherence tomography (SD-OCT) images were obtained using an Envisu R2200-HR SD-OCT instrument (Bioptigen, Durham, NC). [20, 48] Each eye was imaged using linear horizontal scans in the temporal and nasals quadrants and linear vertical scans in the superior and inferior quadrants.

Image Processing and Segmentation

SD-OCT scans were processed and segmented as previously reported. [20, 48] Briefly, SD-OCT scans were converted into image files using ImageJ (version 1.48; National Institutes of Health, Bethesda, MD) and, using a custom designed SD-OCT segmentation program built in IGOR Pro (IGOR Pro 6.37; WaveMetrics Inc., Lake Oswego, OR), total retinal (TR) and receptor plus (REC+) thicknesses were measured. [20, 48, 49] The thickness from Bruch's membrane to the vitreous/retinal nerve fiber layer interface is defined as TR. REC+ is defined as the thickness from Bruch's membrane to the inner nuclear layer/outer plexiform layer interface. [20, 48, 49]

Electroretinograms (ERGs)

ERGs were performed as previously reported. [20, 50, 51] ERGs were recorded two to seven days after SD-OCT imaging. Dark-adapted mice were anesthetized with ketamine (100 mg/kg)/xylazine (10 mg/kg), corneas were anesthetized, and pupils were dilated. Mice were placed on a heated platform (37°C) inside of a Ganzfeld dome coated with a highly reflective paint. Platinum signal electrodes were placed on the center of each cornea, and additional electrodes were placed in the forehead and tail as reference and ground, respectively. Finally, a lubricant, Goniovisc, Hypromellose 2.5% (Dynamic Diagnostics, Westland, MI), was applied to the corneas. ERG traces were averaged and analyzed using custom software. Light intensities ranged from -4.34 to 3.55 log cd•s/m^2. [20, 50, 51] The number of trials at each light intensity was decreased as the intensity of the flashes increased in order to prevent light adaptation. The time between each flash was increased to allow for pigment regeneration. The minimum interstimulus interval was seven seconds, and the maximum was 70 seconds. Flashes were calibrated as previously described. [20, 50, 51]

RNA Extraction and RT-qPCR

Two hours into the 12-hour dark cycle, mice were injected intraperitoneally (10 mL/kg) under dim red light. Mice were dosed with vehicle or 15 mg/kg flibanserin 48 hours, 24 hours and immediately prior to a one-hour bright light exposure, and 24 and 48 hours after light exposure. Retinas from vehicle-injected mice and flibanserin-injected mice were harvested 48 hours and 72 hours after light exposure. Total RNA was extracted from retinas using an RNeasy Mini Kit (Qiagen, Hilden, Germany). One microgram of total RNA was converted to cDNA using a Bio-Rad iScript cDNA synthesis kit (Hercules, CA). Primers were designed with the Integrated DNA Technologies Realtime PCR Tool (S1 Table, Coralville, Iowa). PCR reaction mixtures consisted of 10 μL DyNAmo HS SYBR green (Thermo Scientific, Waltham, MA), 1 μL cDNA template, 1 μL of 200 μM gene-specific primer sets, and 8 μL distilled water. Using a Bio-Rad Chromo4 System (Hercules, CA), samples were initially denatured for 2 minutes at 95°C, followed by 40 cycles at 95°C for 15 seconds and 58°C for 30 seconds. Gene expression was normalized to β-actin and relative gene expression in flibanserin-injected mice was compared to vehicle-injected mice using the ΔΔCt method.

Statistical Analysis

Average outer retinal thickness (REC+), total retinal thickness (TR), a-wave amplitudes and b-wave amplitudes were calculated for each animal. Representative topographic distributions were an average of the REC+ thicknesses from the right eyes for all animals in each group, centered at the optic nerve. For scatterplot graphs, left and right eye data was combined for each animal and then averaged for each group. One-way analysis of variance (ANOVA) was used to compare REC+, TR and three different ERG measurements: $b_{max,rod}$ at -2.14 log cd•s/m^2, and $a_{max,rod+cone}$ and $b_{max,rod+cone}$ at 3.55 log cd•s/m^2 using Prism (Prism 6.0; GraphPad Software Inc., La Jolla, CA). Multiple t-tests were performed to compare the expression of individual genes in flibanserin- and vehicle-injected mice at 48- and 72-hours after light exposure. For all analyses, a *P* value less than 0.05 was considered significant.

Results

Flibanserin-Mediated Neuroprotection

Five-day time course. Bright light exposure resulted in thinning of the outer nuclear layer (ONL) and obscuration of the inner segment/outer segment junction (IS/OS) in retinas of

vehicle-injected mice, and 0.75 and 1.5 mg/kg flibanserin-injected mice, as compared the normal morphology of naïve mice (Fig 1A). Injections with 3, 6, 9, and 15 mg/kg of flibanserin not only preserved the ONL and IS/OS, but also revealed a dose-dependent preservation of ONL thickness (Fig 1A and 1B). Average REC+ thicknesses of 3, 6, 9, and 15 mg/kg flibanserin were significantly increased from vehicle-treated mice (Table 1, Fig 1B), and administration of 15 mg/kg flibanserin provided maximum protection of retinal morphology, resulting in non-significant differences in REC+ thickness as compared to non-light damaged naïve mice.

ERGs demonstrated severe attenuation of retinal function in vehicle-injected mice versus naïve mice, as observed in the representative ERG waveforms and scotopic a-wave and b-wave amplitudes (Fig 2A and 2B, S1A Fig, Table 2). Intensity response curves and average a- and b-wave amplitudes highlight the variable protection between treatment groups and a general dose-dependent effect (Fig 2B). 15 and 9 mg/kg flibanserin groups were not significantly different from the naïve group in b-wave responses ($b_{max,rod}$, $b_{max,rod+cone}$), or a-wave responses ($a_{max,rod+cone}$) (Fig 2B, S1A Fig, Table 2). The 1.5 and 0.75 mg/kg flibanserin groups failed to preserve retinal function entirely; ERG responses were not significantly increased from vehicle-injected mice. The 3 mg/kg and 6 mg/kg flibanserin-treated mice showed variable protection in ERG responses, but generally showed reduction of responses from naïve mice but improved from vehicle-treated mice.

One-day time course. In order to ascertain whether flibanserin has the ability to act quickly and effectively, a one-day time course was evaluated. A single dose of 3, 6, 9 or 15 mg/kg flibanserin was injected immediately before light damage. Mice that received a 15, 9 or 6 mg/kg dose of flibanserin displayed complete morphological protection as assessed by OCT, and no statistical difference was found between their average REC+ thicknesses and those of naïve animals (Fig 3A, Table 1). Interestingly, a single injection of 3 mg/kg flibanserin failed to protect retinal morphology, as REC+ thickness was not statistically different from the vehicle-injected mice.

In regard to retinal function, all responses ($b_{max,rod}$, $b_{max,rod+cone}$, and $a_{max,rod+cone}$) for the 6, 9 and 15 mg/kg flibanserin groups were statistically increased from the vehicle-treated group (Fig 3B, S1B Fig, Table 2). A single 3 mg/kg flibanserin injection failed to protect retinal function, thus corresponding with OCT results.

Mechanism of Flibanserin-Mediated Neuroprotection

5-HT_{1A} receptor-mediated neuroprotection. Because flibanserin is both a 5-HT_{1A} agonist and a 5-HT_{2A} antagonist, both receptors may play a role in flibanserin-mediated neuroprotection. However, literature suggests that flibanserin's mechanism of action is primarily due to stimulation of 5-HT_{1A} receptors. [33–39] To investigate the relative contribution of 5-HT_{1A} versus 5-HT_{2A} receptor occupancy in flibanserin-mediated neuroprotection, we utilized both a pharmacologic blockade of 5-HT_{1A} receptors and 5-HT_{1A} knockout mice. Pharmacologic blockade with 10 mg/kg WAY 100635, a 5-HT_{1A} antagonist, was administered to BALB/c mice 30 minutes prior to a single dose of 6 mg/kg flibanserin. As previously observed, a single injection of 6 mg/kg flibanserin in BALB/c mice preserved REC+ thickness (Figs 3A and 4A) and ERG a- and b-wave responses to the level of naïve mice (Figs 3B and 4B, S1B Fig). Pre-treatment with 10 mg/kg WAY 100635 prior to 6 mg/kg flibanserin resulted in a significant, albeit incomplete, reduction in REC+ thickness and ERG a- and b-wave values, as they were significantly less than naïve and 6 mg/kg flibanserin treated mice, but were significantly greater than vehicle-treated mice (Fig 4A and 4B, S1C Fig). To further delineate the necessity of 5-HT_{1A} in flibanserin-mediated neuroprotection, 6 mg/kg flibanserin was administered to 5-HT_{1A} knockout mice. In line with our pharmacologic findings, loss of 5-HT_{1A}

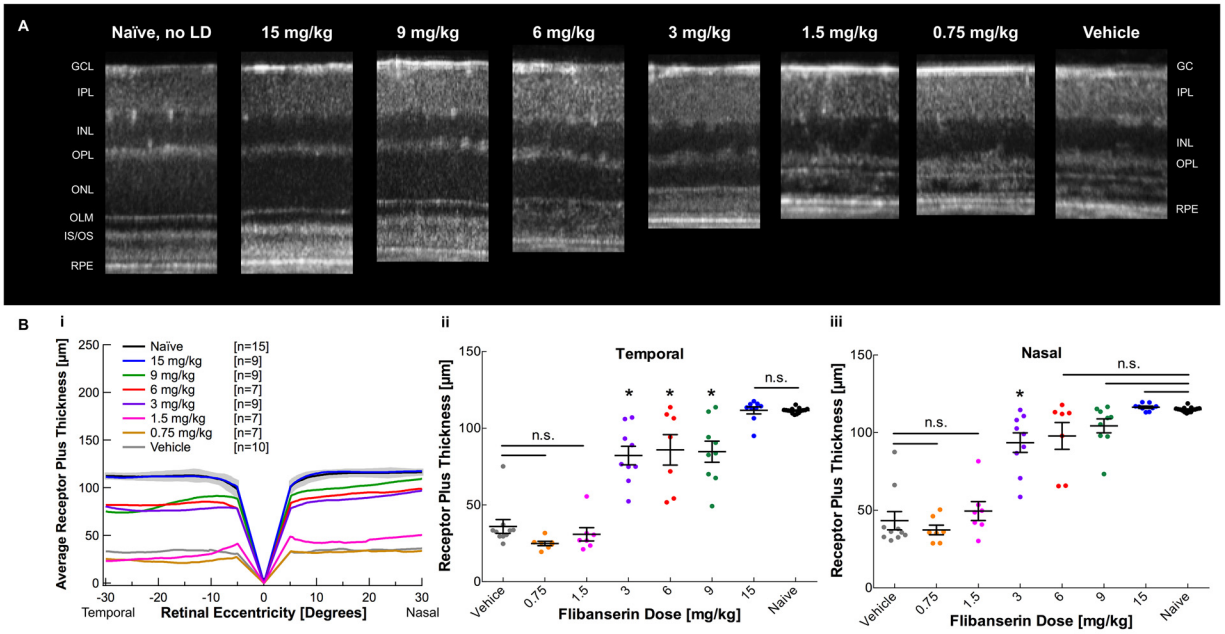

Fig 1. A 5-day time course of flibanserin protects retinal morphology from bright light exposure in a dose-dependent manner. (**A**) Representative linear SD-OCT scans of nasal retina show increasing outer nuclear layer thickness with flibanserin treatment, in a dose-dependent manner. A naïve non-light damaged mouse shows an easily distinguishable OPL, ONL, OLM, IS/OS, and RPE. GCL-ganglion cell layer, IPL-inner plexiform layer, INL-inner nuclear layer, OPL-outer plexiform layer, ONL-outer nuclear layer, OLM-outer limiting membrane, IS/OS-inner segment/outer segment junction, RPE-retinal pigment epithelium. (**B i**) A spider graph of average right-eye receptor plus values demonstrates that flibanserin-mediated protection increases in a dose-dependent manner starting at 3 mg/kg, with a 15 mg/kg dose showing comparable receptor plus thicknesses to naïve (non-light damaged) mice. The gray area indicates ± 2 SD of the naïve averaged data. (**B ii, iii**) Receptor plus thicknesses, with each dot representing average right and left eye thickness from one mouse, demonstrate that 15 mg/kg flibanserin achieves complete morphological protection in the **(B ii)** temporal quadrant and the **(B iii)** nasal quadrant. Group averages are represented as mean ± standard error bar. * indicates a significant difference from both the vehicle-treated group and the naïve group, $P < 0.05$. n.s. indicates non-significance with $P > 0.05$.

doi:10.1371/journal.pone.0159776.g001

Table 1. Summary of OCT findings.

		Nasal		Temporal	
Group	***n***	**TR (µm) Mean ± SD**	**Rec+ (µm) Mean ± SD**	**TR (µm) Mean ± SD**	**Rec+ (µm) Mean ± SD**
Five-day Time Course					
Vehicle	10	125 ± 18	43 ± 19	117 ± 14	36 ± 14
Flibanserin, 0.75 mg/kg	7	119 ± 8	37 ± 8	106 ± 4	25 ± 4
Flibanserin, 1.5 mg/kg	7	132 ± 16	50 ± 16	113 ± 13	31 ± 11
Flibanserin, 3 mg/kg	9	175 ± 20	94 ± 19	165 ± 19	82 ± 18
Flibanserin, 6 mg/kg	7	179 ± 23	98 ± 23	168 ± 26	86 ± 26
Flibanserin, 9 mg/kg	9	185 ± 14	104 ± 14	166 ± 21	85 ± 21
Flibanserin, 15 mg/kg	9	196 ± 3	116 ± 2	191 ± 7	112 ± 7
Naive	15	195 ± 2	115 ± 2	191 ± 2	112 ± 2
One-day Time Course					
Vehicle	7	136 ± 22	52 ± 21	119 ± 18	37 ± 17
Flibanserin, 3 mg/kg	5	120 ± 12	39 ± 11	116 ± 21	36 ± 19
Flibanserin, 6 mg/kg	6	194 ± 3	116 ± 2	192 ± 3	112 ± 2
Flibanserin, 9 mg/kg	6	199 ± 2	120 ± 2	196 ± 2	118 ± 3
Flibanserin, 15 mg/kg	7	197 ± 3	114 ± 2	194 ± 3	111 ± 2
Naive	15	195 ± 2	115 ± 2	191 ± 2	112 ± 2

doi:10.1371/journal.pone.0159776.t001

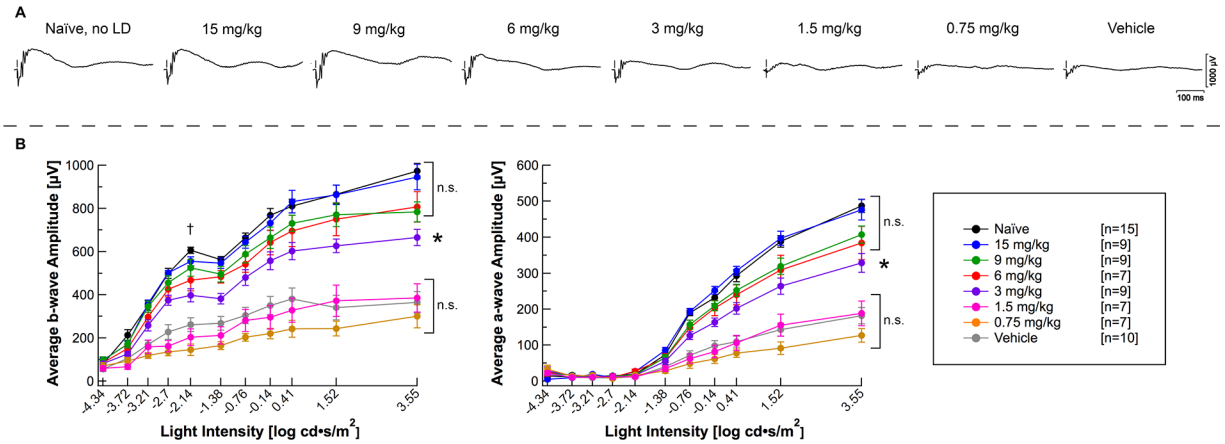

Fig 2. A 5-day time course of flibanserin preserves retinal function in a dose-dependent manner, as measured by ERG. (**A**) Representative ERG traces at the 3.55 log cd•s/m^2 light intensity demonstrating dose-dependent improvements in ERG responses as compared to vehicle-injected mice. (**B**) Mice treated with doses of 3 mg/kg or greater of flibanserin showed significantly higher ERG b-wave and a-wave responses at the highest ERG flash intensity (3.55 log cds/m^2) as compared to vehicle-treated mice. Individual ERGs were averaged with ERGs for mice within its respective group and are represented as mean ± standard error. * indicates a significant difference from both the vehicle-treated group and the naïve group, $P < 0.05$. n.s. indicates non-significance with $P > 0.05$. The responses at the ERG $b_{(max,rod)}$ light intensity, indicated by the "†", were statistically evaluated and are represented in S1A Fig.

doi:10.1371/journal.pone.0159776.g002

almost completely negated the protective effect of flibanserin from light-induced retinopathy (Fig 4A and 4B, S1C Fig).

Augmentation of genes involved in cell survival. Potential cell survival mechanisms involved in flibanserin-mediated neuroprotection were assessed via reverse transcription-quantitative PCR (RT-qPCR); specifically, genes involved with the inhibition of apoptosis or reduction of reactive oxygen species were evaluated. At 48-hours post-light exposure, flibanserin treatment significantly increased gene expression of cAMP response element-binding protein (*Creb*, 5.0-fold), B-cell lymphoma 2 (*Bcl-2*, 3.7-fold), Calpastatin 1 (*Cast1*, 4.2-fold),

Table 2. Summary of ERG parameters.

Group	*n*	$b_{max,rod}$ (μV) Mean ± SD	$a_{max,rod+cone}$ (μV) Mean ± SD	$b_{max,rod+cone}$ (μV) Mean ± SD
Five-day Time Course				
Vehicle	10	262 ± 99	181 ± 71	365 ± 155
Flibanserin, 0.75 mg/kg	7	146 ± 70	127 ± 50	301 ± 142
Flibanserin, 1.5 mg/kg	7	203 ± 104	189 ± 91	386 ± 174
Flibanserin, 3 mg/kg	9	398 ± 91	329 ± 80	666 ± 114
Flibanserin, 6 mg/kg	7	468 ± 131	384 ± 123	807 ± 186
Flibanserin, 9 mg/kg	9	525 ± 118	407 ± 71	785 ± 139
Flibanserin, 15 mg/kg	9	556 ± 64	476 ± 86	945 ± 177
Naive	15	606 ± 58	487 ± 68	973 ± 129
One-day Time Course				
Vehicle	7	251 ± 47	229 ± 51	424 ± 101
Flibanserin, 3 mg/kg	5	226 ± 87	167 ± 88	393 ± 167
Flibanserin, 6 mg/kg	5	579 ± 93	466 ± 118	917 ± 187
Flibanserin, 9 mg/kg	6	464 ± 73	357 ± 110	668 ± 284
Flibanserin, 15 mg/kg	7	513 ± 65	459 ± 53	934 ± 121
Naive	15	606 ± 58	487 ± 68	973 ± 129

doi:10.1371/journal.pone.0159776.t002

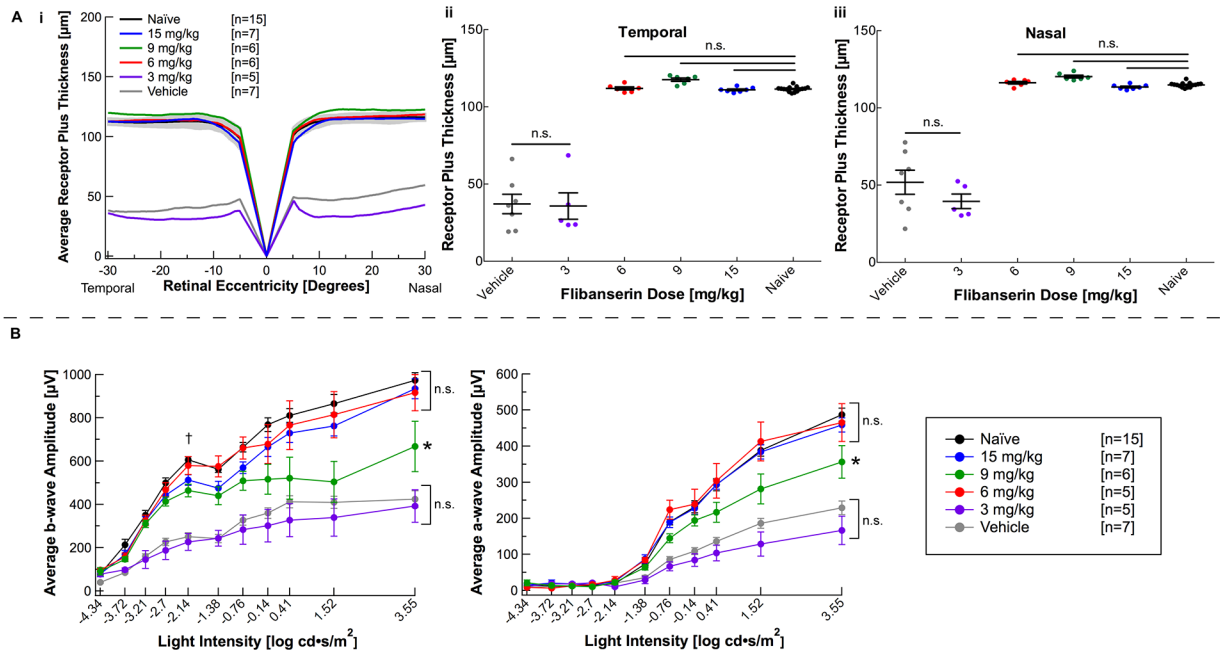

Fig 3. A one-day time course of flibanserin can preserve retinal morphology and function. (A i) A spider graph representing average right-eye receptor plus values demonstrates that a single dose of 6 mg/kg flibanserin or greater can significantly preserve retinal morphology to thicknesses comparable to naïve mice. The gray area indicates ± 2 SD of the naïve averaged data. (**A ii, iii**) Receptor plus thicknesses, with each dot representing average right and left eye thickness from one mouse, demonstrate that 6 mg/kg flibanserin provides morphological protection in the **(A ii)** temporal quadrant and the **(A iii)** nasal quadrant. Group averages are represented as mean ± standard error bar. **(B)** Mice treated with doses of 6 mg/kg and greater of flibanserin showed significantly higher ERG b-wave and a-wave responses at the highest flash intensity (3.55 log cd•s/m^2) as compared to vehicle-treated mice. "†" indicates the greatest flash intensity that elicits a rod-only response ($b_{(max,rod)}$). Group differences at the "†" flash intensity were statistically evaluated and are represented in S1B Fig. Individual ERGs were averaged with ERGs for mice within group and are represented as mean ± standard error. * indicates a significant difference from both the vehicle-treated group and the naïve group, $P < 0.05$. n.s. indicates non-significance with $P > 0.05$.

doi:10.1371/journal.pone.0159776.g003

Superoxide dismutase 1 (*Sod1*, 3.8-fold), and Catalase (*Cat*, 6.9-fold) compared to vehicle treatment (Fig 5A). Similarly, 72-hours post-light exposure, flibanserin significantly increased the gene expression of *Creb* (2.4-fold), *Bcl-2* (3.0-fold), *Cast1* (2.4-fold), and *Sod1* (2.1-fold) versus vehicle (Fig 5B). Additionally, *c-Jun* (3.1-fold), *c-Fos* (2.5-fold), and NAD(P)H quinone dehydrogenase 1 (*Nqo1*, 2.4-fold) were significantly increased in flibanserin-injected mice compared to vehicle-injected mice.

Discussion

This research demonstrates the novel finding that flibanserin, a dual serotonin receptor agonist and antagonist recently approved by the United States Food and Drug Administration for female HSDD, can completely protect the structural and functional integrity of albino BALB/c mouse retinas from light-induced retinopathy. Flibanserin's neuroprotective effects began with a 3 mg/kg dose following a five-day time course and a 6 mg/kg dose following a one-day time course. A 15 mg/kg dose of flibanserin, following either time course, fully prevented the photoreceptor degeneration caused by bright light exposure.

Filbanserin demonstrated neuroprotection in a dose-dependent manner, consistent with the known pharmacokinetics of the drug. Borsini et al. showed that in the cortex, the 20% minimum receptor occupancy required for 5-HT_{1A} receptor activation was reached after a single 1 mg/kg dose, but that a 10 mg/kg dose was required to reach the same level of receptor occupancy in the

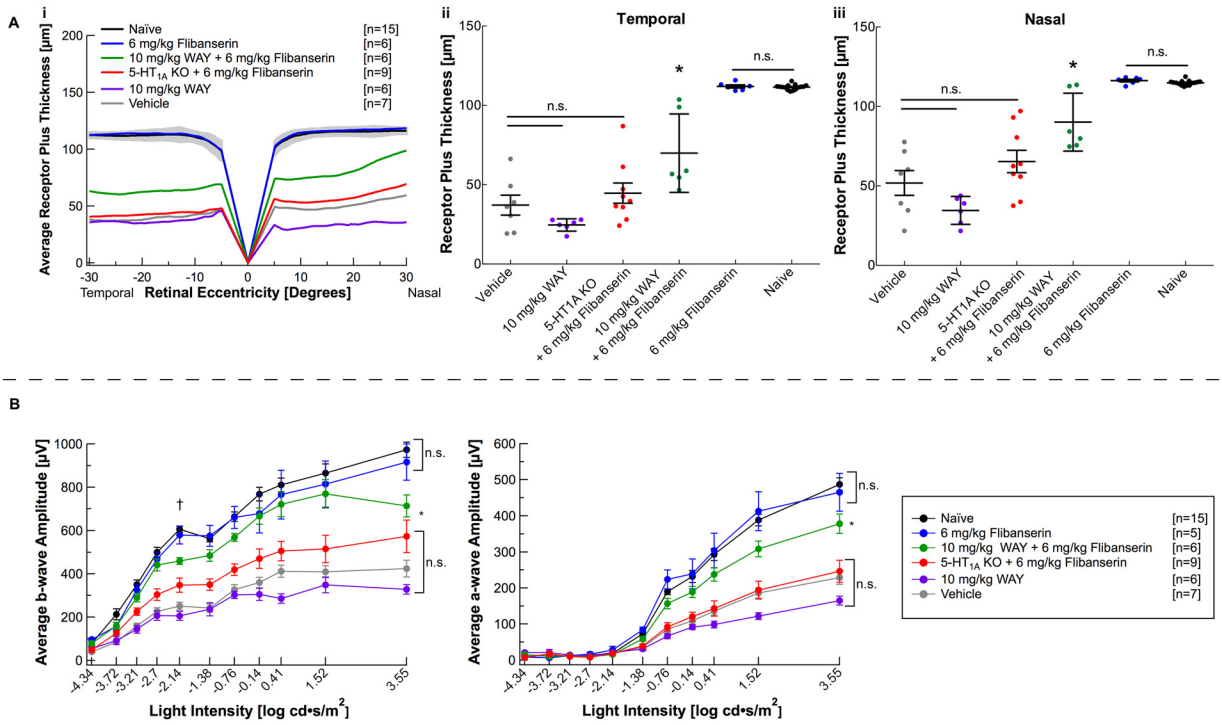

Fig 4. Flibanserin's neuroprotective effects are 5-HT$_{1A}$ receptor-mediated. (**A i**) A spider graph representing average right-eye receptor plus values demonstrates that pre-treatment with WAY 100635 prior to 6 mg/kg flibanserin (10 mg/kg WAY + 6 mg/kg Flibanserin, *green*) decreased average receptor plus thickness as compared to flibanserin-treatment without WAY 100635 (6 mg/kg Flibanserin, *blue*). A 6 mg/kg dose of flibanserin in 5-HT$_{1A}$ knockout mice (5-HT1A KO + 6 mg/kg Flibanserin, *red*) resulted in average receptor plus thickness that was not significantly different from vehicle-injected and naïve mice. The gray area indicates ± 2 SD of the naïve averaged data. (**A ii, A iii**) Receptor plus thicknesses, with each dot representing average right and left eye thickness from one mouse, demonstrate that both pre-treatment of BALB/c mice with WAY 100635 prior to a flibanserin injection (10 mg/kg WAY + 6 mg/kg Flibanserin, *green*) and a flibanserin injection in 5-HT$_{1A}$ knockout mice (5-HT1A KO + 6 mg/kg Flibanserin, *red*) significantly reduces the observed neuroprotective effects provided by a single 6 mg/kg dose of flibanserin (6 mg/kg Flibanserin, *blue*) in the **(A ii)** temporal quadrant and the **(A iii)** nasal quadrant. (**B**) Pre-treatment with WAY 100635 (10 mg/kg WAY + 6 mg/kg Flibanserin, *green*) mitigated the improvements to ERG a- and b-wave amplitudes provided by a single 6 mg/kg dose of flibanserin (*blue*). ERG a- and b-wave amplitudes were not improved by a single dose of 6 mg/kg flibanserin when administered to 5-HT$_{1A}$ knockout mice (5-HT1A KO + 6 mg/kg Flibanserin, *red*). "†" indicates the flash intensity providing the b$_{(max,rod)}$ value at which statistical analyses was also performed and presented in S1C Fig. * indicates a significant difference from both the vehicle-treated group and the naïve group, $P < 0.05$. n.s. indicates non-significance with $P > 0.05$.

doi:10.1371/journal.pone.0159776.g004

hippocampus and dorsal raphe. [34] The dose needed to occupy receptors in the retina is currently unknown, but based on the finding that a single administration of 6 mg/kg or more was required to achieve neuroprotection, we hypothesize that the occupancy of 5-HT$_{1A}$ receptors needed for neuroprotection in the retina is closer to that of the hippocampus and dorsal raphe.

In humans, three daily-administrations of flibanserin are required for the drug to reach steady state plasma concentrations. [33] The time to reach steady state concentrations of flibanserin is currently unknown in mice. However, due to flibanserin's differing half-life in humans (11 hours) versus rats (0.9 to 1.9 hours), the time to reach steady state concentrations in rodents likely takes longer than three days. [34] Since flibanserin was only injected three times prior to light damage, maximum plasma and retinal concentrations may not have been reached with lower doses. Therefore, we hypothesize that if the number of daily-injections prior to light damage was increased, the total concentration of flibanserin would also increase, subsequently enhancing the neuroprotective effects of even the low doses.

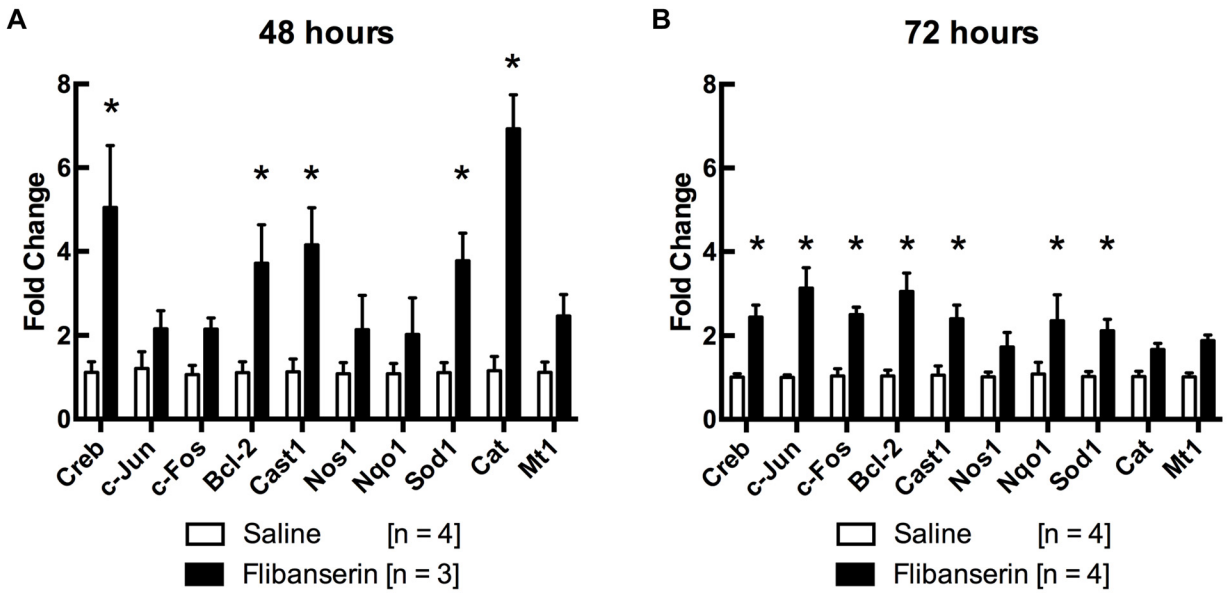

Fig 5. Flibanserin increases anti-apoptotic and antioxidant gene expression. (A) RT-qPCR shows that 48 hours following light-exposure, expression of *Creb*, *Bcl-2*, *Cast1*, *Sod1*, and *Cat* are significantly increased in flibanserin-injected mice versus vehicle-injected mice. **(B)** After 72 hours, expression of *Creb*, *c-Jun*, *c-Fos*, *Bcl-2*, *Cast1*, *Nqo1*, and *Sod1* are significantly increased in flibanserin-injected mice versus vehicle-injected mice. Analysis was performed using the ΔΔCt method with β-actin as the internal control. Significance was determined using a multiple t-test analysis (* indicates $P < 0.05$). cAMP Response Binding-element Protein (*Creb*), Cyclin D1 (*Cd1*), B-cell lymphoma 2 (*Bcl-2*), Calpastatin (*Cast1*), Nitric Oxide Synthase (*Nos1*), NAD(P)H quinone dehydrogenase 1 (*Nqo1*), Superoxide Dismutase 1 (*Sod1*), Catalase (*Cat*), Metallothionein 1 (*Mt1*).

doi:10.1371/journal.pone.0159776.g005

Flibanserin has high affinity for the 5-HT_{1A} receptor (K_i = 1 nM) and a lower affinity for the 5-HT_{2A} receptor (K_i = 49nM), but lacks significant affinity for all other serotonergic and adrenergic receptors, allowing for the characterization of the neuroprotective targets, 5-HT_{1A} and 5-HT_{2A}, in combination. [15–20, 22–26, 34] Flibanserin does, however, have moderate affinity for the dopaminergic D_4 receptor (K_i = 4–24 nm), where it acts as an antagonist at low doses, and a partial agonist at higher doses. [34] It has been reported that D_4 receptor agonists can inhibit oxidative stress-induced nerve cell death and protect against hypoxia/reoxygenation-induced cell death in cultured HT22 cells, which suggests that activation of the D_4 receptor could be neuroprotective. [52, 53] Although D_4 receptors have been reported in rodent retina, the threshold at which flibanserin begins functioning as a dopaminergic agonist is not well described in the mouse. [34, 54] Taken together, we considered the possibility that flibanserin-mediated neuroprotection could be due to D_4 receptor activation, but our results suggested otherwise. WAY 100635, a 5-HT_{1A} antagonist and a potent D_4 agonist, was tested in our light-induced retinopathy model, as it binds the D_4 receptor with similar affinity (K_i = 16) as flibanserin. [34, 47] WAY 100635 failed to protect BALB/c retinas, both structurally and functionally, from light-induced retinopathy when given at a molar equivalent dose of the most effective dose of flibanserin, 15 mg/kg (Fig 4A and 4B, S1C Fig). Because this degree of D_4 receptor activation did not protect the retina, it suggests that the observed neuroprotective effects of flibanserin are not likely mediated through D_4 receptors.

In HSDD, Flibanserin is thought to mediate its effect through modulation of serotonin, dopamine and norepinephrine levels in brain regions involved in activating dopaminergic reward and sexual cue integration. [33, 35] Several studies suggest that Flibanserin's action in the brain occurs through 5-HT_{1A} serotonin receptors. [34, 38, 39] This is supported by the finding that WAY 100635, a selective 5-HT_{1A} antagonist, completely antagonized the effects of

flibanserin on serotonin, dopamine and noradrenaline in the rat prefrontal cortex. [35] Our results similarly suggest that flibanserin's neuroprotective effects on the retina are mediated through the 5-HT_{1A} receptor. A single 10 mg/kg dose of WAY 100635 injected 30 minutes prior to a single 6 mg/kg injection of flibanserin severely reduced observed neuroprotective effects. In addition, 6 mg/kg of flibanserin failed to protect the retina from light-induced retinopathy in 5-HT_{1A} knockout mice. Whether flibanserin elicits any effect via the 5-HT_{2A} receptor remains to be elucidated.

The signaling cascade involved in 5-HT_{1A}-mediated neuroprotection has yet to be fully characterized, therefore we performed gene expression assays to elicit the mechanisms responsible for flibanserin-mediated neuroprotection. The cell death signaling implicated in light-induced retinopathy involves the activation of nitric oxide synthase (*NOS*), increased intracellular calcium, disturbed mitochondrial function, and generation of oxidative stress, all of which can play a role in photoreceptor cell death in inherited retinal degeneration. [40, 55, 56] RT-qPCR results suggest that flibanserin provides neuroprotection by addressing the latter two components. In regard to mitochondrial dysfunction, the upregulation of Calpastatin (*Cast1*) and B-cell lymphoma 2 (*Bcl-2*) may lead to increased cell survival. Calpastatin is an endogenous inhibitor of calpains, which have been linked to caspase-dependent and caspase-independent cell death. [40, 57, 58] Arroba et al. demonstrated that maintained *Cast1* expression, via treatment with insulin-like growth factor-I (IGF-I), can significantly reduce apoptosis. [59] This effect was shown in both 661W cone cells and C57BL/6 mouse retinal explants grown in the presence of excess Ca^{2+}, as well as in naïve rd1 mouse retinal explants. [59] *Bcl-2* has been described as an inhibitor of mitochondrial dysfunction during programmed cell death. [60] Additionally, transgenic expression of *Bcl-2* under control of the rhodopsin promoter has been shown to provide retinal neuroprotection in a light-induced retinopathy model, *rd1* mice, and S334ter-*Rho* mice. [61, 62]

Mitochondrial dysfunction often leads to oxidative stress, which occurs when reactive oxygen species capacity outweighs the antioxidant defense capacity. [63] Accordingly, antioxidants have been evaluated in several light-induced and inherited retinal dystrophy models, and have established their worth as neuroprotective agents. [17, 64–68] Flibanserin's ability to upregulate antioxidant genes may play a significant role in cell survival. [40, 69] We have shown that flibanserin increases expression of Superoxide dismutase 1 (*Sod1*), Catalase (*Cat*), and NAD(P)H quinone dehydrogenase 1 (*Nqo1*). *Sod1* is an antioxidant responsible for the decomposition of free superoxide radicals to molecular oxygen and hydrogen peroxide, while *Cat* reduces the membrane-permeable hydrogen peroxide to water. [70, 71] *Nqo1*, activated by the transcription factor Nrf2, is responsible for quinone detoxification. [72–74] *Nqo1* operates by reducing ROS-generating quinones to hydroquinones, and has been reported to scavenge superoxides directly. [72, 75, 76] All three of these antioxidants have been able to provide protection against oxidative stress. For example, exogenous *Sod1* and *Cat* provided protection against retinal ischemic injury following increased intraocular pressure in different *in vivo* models. [77, 78] Adenovirus-mediated delivery of *Cat* was able to protect RPE cells from hydrogen peroxide-induced oxidative stress, as well as photoreceptors in an *in vivo* light damage model. [71] Additionally, *Nqo1* has played a prominent role in neuroprotection against oxidative stress in neuronal HT22 cells. [79]

Flibanserin treatment also led to significant increases in *c-Jun* and *c-Fos*. As a heterodimer, these proteins assemble into activator protein complex-1 (AP1), a transcription factor closely associated with apoptosis. [80] However, the role of the *c-Fos*/*c-Jun* heterodimer in apoptosis is complex. [80–82] While studies have shown that light-induced retinopathy can be prevented by the ablation of *c-fos*,[40, 56] this phenomenon only occurs in mice with a methionine substitution at RPE65 codon 450 and not in BALB/c mice which have a leucine mutation at this

position. [82] Knocking out *c-fos* also did not prevent cell death in *rd1* mice. [56] Contrastingly, *c-Fos* and *c-Jun* have also been demonstrated to be anti-apoptotic. Gu et al. reported an absence of AP1 in dying photoreceptors, which argues against its role in photoreceptor apoptosis. AP1 activation was instead observed in Müller cells after light exposure, suggesting a pro-survival effect. [82]

In summary, when light-damage occurs, there is an increase of intracellular calcium, disruption of mitochondrial function, and oxidative stress. [40] We hypothesize that flibanserin treatment leads to the activation of *Creb*, which can upregulate *Cast1* and *Bcl-2* and protect against mitochondrial dysfunction. Furthermore, *Bcl-2* has the ability to modulate cellular calcium concentrations and increase antioxidant genes, such as *Sod1*, *Cat* and *NqO1*. [40, 60, 83–85] Although we saw a flibanserin-mediated increases in *c-Fos* and *c-Jun*, the role they play in neuroprotection remains unclear.

Flibanserin was recently approved by the FDA and marketed as Addyi™ for the treatment of HSDD and its side effects are relatively benign in both men and women; the most frequent adverse events being dizziness, somnolence, nausea and fatigue. [29] The potential to repurpose flibanserin for retinal neuroprotection is exciting. However, much work remains to transition it into a viable treatment for inherited retinal dystrophies, such as evaluation of its neuroprotective effects in an animal model of inherited retinal degeneration. Other avenues of delivery, such as intraocular injection, could also be explored to reduce possible systemic side effects. With its documented safety profile and FDA-approved status, further investigation of flibanserin for the treatment of retinal degenerations is warranted.

Supporting Information

S1 Fig. Statistical analyses of ERG b-wave responses at the $b_{(max,\ rod)}$ response. (**A**) Five daily-doses of 3 mg/kg flibanserin and greater preserve the ERG $b_{(max,\ rod)}$ response. (**B**) A single dose of 6 mg/kg flibanserin or greater can preserve the ERG $b_{(max,\ rod)}$ response. (**C**) The ERG $b_{(max,\ rod)}$ response observed after a single dose of 6 mg/kg flibanserin was significantly reduced in both 5-HT_{1A} knockout mice (5-HT1A KO + 6 mg/kg Flibanserin, *red*) and mice that received a pre-treatment of WAY 100635 (10 mg/kg WAY + 6 mg/kg Flibanserin, *green*). The averaged right and left eye data for each mouse is represented as a dot. Group averages are represented as mean ± standard error bar. * indicates a significant difference from both the vehicle-treated group and the naïve group, $P < 0.05$. n.s. indicates non-significance with $P > 0.05$.
(TIF)

S1 Table. Primers for RT-qPCR.
(DOCX)

Author Contributions

Conceived and designed the experiments: ASC RCR CAK MEP. Performed the experiments: ASC. Analyzed the data: ASC CMF RCP SD. Contributed reagents/materials/analysis tools: MEP PY. Wrote the paper: ASC RCR CAK. Designed the software used in analysis: YW. Provided 5-HT1A knockout mice: RH.

References

1. Hamel CP. Gene discovery and prevalence in inherited retinal dystrophies. C R Biol. 2014; 337 (3):160–6. doi: 10.1016/j.crvi.2013.12.001 PMID: 24702842.

2. Kohl S, Biskup S. [Genetic diagnostic testing in inherited retinal dystrophies]. Klin Monbl Augenheilkd. 2013; 230(3):243–6. doi: 10.1055/s-0032-1327929 PMID: 23208805.
3. Nentwich MM, Rudolph G. Hereditary retinal eye diseases in childhood and youth affecting the central retina. Oman J Ophthalmol. 2013; 6(Suppl 1):S18–25. doi: 10.4103/0974-620X.122290 PMID: 24391367; PubMed Central PMCID: PMCPMC3872838.
4. Bainbridge JW, Smith AJ, Barker SS, Robbie S, Henderson R, Balaggan K, et al. Effect of gene therapy on visual function in Leber's congenital amaurosis. N Engl J Med. 2008; 358(21):2231–9. doi: 10.1056/NEJMoa0802268 PMID: 18441371.
5. Hauswirth WW, Aleman TS, Kaushal S, Cideciyan AV, Schwartz SB, Wang L, et al. Treatment of leber congenital amaurosis due to RPE65 mutations by ocular subretinal injection of adeno-associated virus gene vector: short-term results of a phase I trial. Hum Gene Ther. 2008; 19(10):979–90. doi: 10.1089/hum.2008.107 PMID: 18774912; PubMed Central PMCID: PMCPMC2940541.
6. Maguire AM, Simonelli F, Pierce EA, Pugh EN Jr., Mingozzi F, Bennicelli J, et al. Safety and efficacy of gene transfer for Leber's congenital amaurosis. N Engl J Med. 2008; 358(21):2240–8. doi: 10.1056/NEJMoa0802315 PMID: 18441370; PubMed Central PMCID: PMCPMC2829748.
7. MacLaren RE, Groppe M, Barnard AR, Cottriall CL, Tolmachova T, Seymour L, et al. Retinal gene therapy in patients with choroideremia: initial findings from a phase 1/2 clinical trial. Lancet. 2014; 383 (9923):1129–37. doi: 10.1016/S0140-6736(13)62117-0 PMID: 24439297; PubMed Central PMCID: PMCPMC4171740.
8. Cideciyan AV, Hauswirth WW, Aleman TS, Kaushal S, Schwartz SB, Boye SL, et al. Human RPE65 gene therapy for Leber congenital amaurosis: persistence of early visual improvements and safety at 1 year. Hum Gene Ther. 2009; 20(9):999–1004. doi: 10.1089/hum.2009.086 PMID: 19583479; PubMed Central PMCID: PMCPMC2829287.
9. Sjoerdsma A, Palfreyman MG. History of serotonin and serotinin disorders. Ann N Y Acad Sci. 1990; 600:1–7; discussion -8. PMID: 2252303.
10. Chanut E, Nguyen-Legros J, Labarthe B, Trouvin JH, Versaux-Botteri C. Serotonin synthesis and its light-dark variation in the rat retina. J Neurochem. 2002; 83(4):863–9. PMID: 12421358.
11. Jin XT, Brunken WJ. Serotonin receptors modulate rod signals: a neuropharmacological comparison of light- and dark-adapted retinas. Vis Neurosci. 1998; 15(5):891–902. PMID: 9764532.
12. Brunken WJ, Jin XT. A role for 5HT3 receptors in visual processing in the mammalian retina. Vis Neurosci. 1993; 10(3):511–22. PMID: 8494802.
13. Mangel SC, Brunken WJ. The effects of serotonin drugs on horizontal and ganglion cells in the rabbit retina. Vis Neurosci. 1992; 8(3):213–8. PMID: 1532124.
14. Oh SJ, Ha HJ, Chi DY, Lee HK. Serotonin receptor and transporter ligands—current status. Curr Med Chem. 2001; 8(9):999–1034. PMID: 11472239.
15. Collier RJ, Patel Y, Martin EA, Dembinska O, Hellberg M, Krueger DS, et al. Agonists at the serotonin receptor (5-HT(1A)) protect the retina from severe photo-oxidative stress. Invest Ophthalmol Vis Sci. 2011; 52(5):2118–26. doi: 10.1167/iovs.10-6304 PMID: 21087971.
16. Collier RJ, Wang Y, Smith SS, Martin E, Ornberg R, Rhoades K, et al. Complement deposition and microglial activation in the outer retina in light-induced retinopathy: inhibition by a 5-HT1A agonist. Invest Ophthalmol Vis Sci. 2011; 52(11):8108–16. doi: 10.1167/iovs.10-6418 PMID: 21467172.
17. Biswal MR, Ahmed CM, Ildefonso CJ, Han P, Li H, Jivanji H, et al. Systemic treatment with a 5HT1a agonist induces anti-oxidant protection and preserves the retina from mitochondrial oxidative stress. Exp Eye Res. 2015; 140:94–105. doi: 10.1016/j.exer.2015.07.022 PMID: 26315784; PubMed Central PMCID: PMCPMC4624518.
18. Thampi P, Rao HV, Mitter SK, Cai J, Mao H, Li H, et al. The 5HT1a receptor agonist 8-Oh DPAT induces protection from lipofuscin accumulation and oxidative stress in the retinal pigment epithelium. PLoS One. 2012; 7(4):e34468. doi: 10.1371/journal.pone.0034468 PMID: 22509307; PubMed Central PMCID: PMCPMC3317995.
19. Inoue-Matsuhisa E, Sogo S, Mizota A, Taniai M, Takenaka H, Mano T. Effect of MCI-9042, a 5-HT2 receptor antagonist, on retinal ganglion cell death and retinal ischemia. Exp Eye Res. 2003; 76(4):445–52. PMID: 12634109.
20. Tullis BE, Ryals RC, Coyner AS, Gale MJ, Nicholson A, Ku C, et al. Sarpogrelate, a 5-HT2A Receptor Antagonist, Protects the Retina From Light-Induced Retinopathy. Invest Ophthalmol Vis Sci. 2015; 56 (8):4560–9. doi: 10.1167/iovs.15-16378 PMID: 26200496; PubMed Central PMCID: PMCPMC4515947.
21. S W, Lu J. A brief summary for 5-HT receptors. Journal of Genetic Syndromes & Gene Therapy. 2013;-4(- 2157–7412):- 1–7.

22. Chen Y, Palczewska G, Mustafi D, Golczak M, Dong Z, Sawada O, et al. Systems pharmacology identifies drug targets for Stargardt disease-associated retinal degeneration. J Clin Invest. 2013; 123 (12):5119–34. doi: 10.1172/JCI69076 PMID: 24231350; PubMed Central PMCID: PMCPMC3859412.

23. Haverkamp S, Inta D, Monyer H, Wassle H. Expression analysis of green fluorescent protein in retinal neurons of four transgenic mouse lines. Neuroscience. 2009; 160(1):126–39. doi: 10.1016/j.neuroscience.2009.01.081 PMID: 19232378.

24. Lu Q, Ivanova E, Pan ZH. Characterization of green fluorescent protein-expressing retinal cone bipolar cells in a 5-hydroxytryptamine receptor 2a transgenic mouse line. Neuroscience. 2009; 163(2):662–8. PMID: 19589372; PubMed Central PMCID: PMCPMC2769501.

25. Pootanakit K, Prior KJ, Hunter DD, Brunken WJ. 5-HT2a receptors in the rabbit retina: potential presynaptic modulators. Vis Neurosci. 1999; 16(2):221–30. PMID: 10367957.

26. Chen Y, Okano K, Maeda T, Chauhan V, Golczak M, Maeda A, et al. Mechanism of all-trans-retinal toxicity with implications for stargardt disease and age-related macular degeneration. J Biol Chem. 2012; 287(7):5059–69. doi: 10.1074/jbc.M111.315432 PMID: 22184108; PubMed Central PMCID: PMCPMC3281612.

27. Du Y, Cramer M, Lee CA, Tang J, Muthusamy A, Antonetti DA, et al. Adrenergic and serotonin receptors affect retinal superoxide generation in diabetic mice: relationship to capillary degeneration and permeability. FASEB J. 2015; 29(5):2194–204. doi: 10.1096/fj.14-269431 PMID: 25667222; PubMed Central PMCID: PMCPMC4415023.

28. Administration USFaD. Background document for meeting of advisory committee for reproductive health drugs-NDA 22-526-flibanserin. 2010.

29. Administration USFaD. Highlights of prescribing information for Addyi (flibanserin). 2015.

30. Derogatis LR, Komer L, Katz M, Moreau M, Kimura T, Garcia M Jr., et al. Treatment of hypoactive sexual desire disorder in premenopausal women: efficacy of flibanserin in the VIOLET Study. J Sex Med. 2012; 9(4):1074–85. doi: 10.1111/j.1743-6109.2011.02626.x PMID: 22248038.

31. Thorp J, Simon J, Dattani D, Taylor L, Kimura T, Garcia M Jr., et al. Treatment of hypoactive sexual desire disorder in premenopausal women: efficacy of flibanserin in the DAISY study. J Sex Med. 2012; 9(3):793–804. doi: 10.1111/j.1743-6109.2011.02595.x PMID: 22239862.

32. Jayne C, Simon JA, Taylor LV, Kimura T, Lesko LM, investigators Ss. Open-label extension study of flibanserin in women with hypoactive sexual desire disorder. J Sex Med. 2012; 9(12):3180–8. doi: 10.1111/j.1743-6109.2012.02942.x PMID: 23057791.

33. Deeks ED. Flibanserin: First Global Approval. Drugs. 2015; 75(15):1815–22. doi: 10.1007/s40265-015-0474-y PMID: 26412054.

34. Borsini F, Evans K, Jason K, Rohde F, Alexander B, Pollentier S. Pharmacology of flibanserin. CNS Drug Rev. 2002; 8(2):117–42. PMID: 12177684.

35. Invernizzi RW, Sacchetti G, Parini S, Acconcia S, Samanin R. Flibanserin, a potential antidepressant drug, lowers 5-HT and raises dopamine and noradrenaline in the rat prefrontal cortex dialysate: role of 5-HT(1A) receptors. Br J Pharmacol. 2003; 139(7):1281–8. doi: 10.1038/sj.bjp.0705341 PMID: 12890707; PubMed Central PMCID: PMCPMC1573953.

36. Borsini F, Giraldo E, Monferini E, Antonini G, Parenti M, Bietti G, et al. BIMT 17, a 5-HT2A receptor antagonist and 5-HT1A receptor full agonist in rat cerebral cortex. Naunyn Schmiedebergs Arch Pharmacol. 1995; 352(3):276–82. PMID: 8584042.

37. Strecker K, Adamaszek M, Ohm S, Wegner F, Beck J, Schwarz J. The 5-HT1A-receptor agonist flibanserin reduces drug-induced dyskinesia in RGS9-deficient mice. J Neural Transm (Vienna). 2012; 119 (11):1351–9. doi: 10.1007/s00702-012-0815-x PMID: 22569849.

38. Scandroglio A, Monferini E, Borsini F. Ex vivo binding of flibanserin to serotonin 5-HT1A and 5-HT2A receptors. Pharmacol Res. 2001; 43(2):179–83. doi: 10.1006/phrs.2000.0762 PMID: 11243720.

39. Borsini F, Brambilla A, Grippa N, Pitsikas N. Behavioral effects of flibanserin (BIMT 17). Pharmacol Biochem Behav. 1999; 64(1):137–46. PMID: 10495008.

40. Wenzel A, Grimm C, Samardzija M, Reme CE. Molecular mechanisms of light-induced photoreceptor apoptosis and neuroprotection for retinal degeneration. Prog Retin Eye Res. 2005; 24(2):275–306. doi: 10.1016/j.preteyeres.2004.08.002 PMID: 15610977.

41. Ueki Y, Wang J, Chollangi S, Ash JD. STAT3 activation in photoreceptors by leukemia inhibitory factor is associated with protection from light damage. J Neurochem. 2008; 105(3):784–96. doi: 10.1111/j.1471-4159.2007.05180.x PMID: 18088375.

42. Zhao L, Wang C, Song D, Li Y, Song Y, Su G, et al. Systemic administration of the antioxidant/iron chelator alpha-lipoic acid protects against light-induced photoreceptor degeneration in the mouse retina. Invest Ophthalmol Vis Sci. 2014; 55(9):5979–88. doi: 10.1167/iovs.14-15025 PMID: 25146987; PubMed Central PMCID: PMCPMC4172298.

43. Song D, Song Y, Hadziahmetovic M, Zhong Y, Dunaief JL. Systemic administration of the iron chelator deferiprone protects against light-induced photoreceptor degeneration in the mouse retina. Free Radic Biol Med. 2012; 53(1):64–71. doi: 10.1016/j.freeradbiomed.2012.04.020 PMID: 22579919; PubMed Central PMCID: PMCPMC3380452.

44. Imai S, Inokuchi Y, Nakamura S, Tsuruma K, Shimazawa M, Hara H. Systemic administration of a free radical scavenger, edaravone, protects against light-induced photoreceptor degeneration in the mouse retina. Eur J Pharmacol. 2010; 642(1–3):77–85. doi: 10.1016/j.ejphar.2010.05.057 PMID: 20553915.

45. Rezaie T, McKercher SR, Kosaka K, Seki M, Wheeler L, Viswanath V, et al. Protective effect of carnosic acid, a pro-electrophilic compound, in models of oxidative stress and light-induced retinal degeneration. Invest Ophthalmol Vis Sci. 2012; 53(12):7847–54. doi: 10.1167/iovs.12-10793 PMID: 23081978; PubMed Central PMCID: PMCPMC3508754.

46. Ramboz S, Oosting R, Amara DA, Kung HF, Blier P, Mendelsohn M, et al. Serotonin receptor 1A knockout: an animal model of anxiety-related disorder. Proc Natl Acad Sci U S A. 1998; 95(24):14476–81. PMID: 9826725; PubMed Central PMCID: PMCPMC24398.

47. Chemel BR, Roth BL, Armbruster B, Watts VJ, Nichols DE. WAY-100635 is a potent dopamine D4 receptor agonist. Psychopharmacology (Berl). 2006; 188(2):244–51. doi: 10.1007/s00213-006-0490-4 PMID: 16915381.

48. Pennesi ME, Michaels KV, Magee SS, Maricle A, Davin SP, Garg AK, et al. Long-term characterization of retinal degeneration in rd1 and rd10 mice using spectral domain optical coherence tomography. Invest Ophthalmol Vis Sci. 2012; 53(8):4644–56. doi: 10.1167/iovs.12-9611 PMID: 22562504; PubMed Central PMCID: PMCPMC3394742.

49. Hood DC, Lin CE, Lazow MA, Locke KG, Zhang X, Birch DG. Thickness of receptor and post-receptor retinal layers in patients with retinitis pigmentosa measured with frequency-domain optical coherence tomography. Invest Ophthalmol Vis Sci. 2009; 50(5):2328–36. doi: 10.1167/iovs.08-2936 PMID: 19011017; PubMed Central PMCID: PMCPMC2835526.

50. Lyubarsky AL, Pugh EN Jr. Recovery phase of the murine rod photoresponse reconstructed from electroretinographic recordings. J Neurosci. 1996; 16(2):563–71. PMID: 8551340.

51. Pennesi ME, Cho JH, Yang Z, Wu SH, Zhang J, Wu SM, et al. BETA2/NeuroD1 null mice: a new model for transcription factor-dependent photoreceptor degeneration. J Neurosci. 2003; 23(2):453–61. PMID: 12533605.

52. Ishige K, Chen Q, Sagara Y, Schubert D. The activation of dopamine D4 receptors inhibits oxidative stress-induced nerve cell death. J Neurosci. 2001; 21(16):6069–76. PMID: 11487630.

53. Shimada S, Hirabayashi M, Ishige K, Kosuge Y, Kihara T, Ito Y. Activation of dopamine D4 receptors is protective against hypoxia/reoxygenation-induced cell death in HT22 cells. J Pharmacol Sci. 2010; 114 (2):217–24. PMID: 20921819.

54. Klitten LL, Rath MF, Coon SL, Kim JS, Klein DC, Moller M. Localization and regulation of dopamine receptor D4 expression in the adult and developing rat retina. Exp Eye Res. 2008; 87(5):471–7. doi: 10.1016/j.exer.2008.08.004 PMID: 18778704; PubMed Central PMCID: PMCPMC2597030.

55. Donovan M, Carmody RJ, Cotter TG. Light-induced photoreceptor apoptosis in vivo requires neuronal nitric-oxide synthase and guanylate cyclase activity and is caspase-3-independent. J Biol Chem. 2001; 276(25):23000–8. doi: 10.1074/jbc.M005359200 PMID: 11278285.

56. Sancho-Pelluz J, Arango-Gonzalez B, Kustermann S, Romero FJ, van Veen T, Zrenner E, et al. Photoreceptor cell death mechanisms in inherited retinal degeneration. Mol Neurobiol. 2008; 38(3):253–69. doi: 10.1007/s12035-008-8045-9 PMID: 18982459.

57. Johnson DE. Noncaspase proteases in apoptosis. Leukemia. 2000; 14(9):1695–703. PMID: 10995018.

58. Wendt A, Thompson VF, Goll DE. Interaction of calpastatin with calpain: a review. Biol Chem. 2004; 385(6):465–72. doi: 10.1515/BC.2004.054 PMID: 15255177.

59. Arroba AI, Wallace D, Mackey A, de la Rosa EJ, Cotter TG. IGF-I maintains calpastatin expression and attenuates apoptosis in several models of photoreceptor cell death. Eur J Neurosci. 2009; 30(6):975–86. doi: 10.1111/j.1460-9568.2009.06902.x PMID: 19723289.

60. Thomenius MJ, Distelhorst CW. Bcl-2 on the endoplasmic reticulum: protecting the mitochondria from a distance. J Cell Sci. 2003; 116(Pt 22):4493–9. doi: 10.1242/jcs.00829 PMID: 14576343.

61. Chen J, Flannery JG, LaVail MM, Steinberg RH, Xu J, Simon MI. bcl-2 overexpression reduces apoptotic photoreceptor cell death in three different retinal degenerations. Proc Natl Acad Sci U S A. 1996; 93 (14):7042–7. PMID: 8692941; PubMed Central PMCID: PMCPMC38932.

62. Bennett J, Zeng Y, Bajwa R, Klatt L, Li Y, Maguire AM. Adenovirus-mediated delivery of rhodopsin-promoted bcl-2 results in a delay in photoreceptor cell death in the rd/rd mouse. Gene Ther. 1998; 5 (9):1156–64. doi: 10.1038/sj.gt.3300733 PMID: 9930315.

63. Mylonas C, Kouretas D. Lipid peroxidation and tissue damage. In Vivo. 1999; 13(3):295–309. PMID: 10459507.

64. Organisciak DT, Darrow RA, Barsalou L, Darrow RM, Lininger LA. Light-induced damage in the retina: differential effects of dimethylthiourea on photoreceptor survival, apoptosis and DNA oxidation. Photochem Photobiol. 1999; 70(2):261–8. PMID: 10461466.

65. Ranchon I, Gorrand JM, Cluzel J, Droy-Lefaix MT, Doly M. Functional protection of photoreceptors from light-induced damage by dimethylthiourea and Ginkgo biloba extract. Invest Ophthalmol Vis Sci. 1999; 40(6):1191–9. PMID: 10235553.

66. Ranchon I, Chen S, Alvarez K, Anderson RE. Systemic administration of phenyl-N-tert-butylnitrone protects the retina from light damage. Invest Ophthalmol Vis Sci. 2001; 42(6):1375–9. PMID: 11328754.

67. Specht S, Leffak M, Darrow RM, Organisciak DT. Damage to rat retinal DNA induced in vivo by visible light. Photochem Photobiol. 1999; 69(1):91–8. PMID: 10063804.

68. Organisciak DT, Darrow RM, Barsalou L, Kutty RK, Wiggert B. Circadian-dependent retinal light damage in rats. Invest Ophthalmol Vis Sci. 2000; 41(12):3694–701. PMID: 11053264.

69. Yang JH, Basinger SF, Gross RL, Wu SM. Blue light-induced generation of reactive oxygen species in photoreceptor ellipsoids requires mitochondrial electron transport. Invest Ophthalmol Vis Sci. 2003; 44 (3):1312–9. PMID: 12601064.

70. Chelikani P, Fita I, Loewen PC. Diversity of structures and properties among catalases. Cell Mol Life Sci. 2004; 61(2):192–208. doi: 10.1007/s00018-003-3206-5 PMID: 14745498.

71. Rex TS, Tsui I, Hahn P, Maguire AM, Duan D, Bennett J, et al. Adenovirus-mediated delivery of catalase to retinal pigment epithelial cells protects neighboring photoreceptors from photo-oxidative stress. Hum Gene Ther. 2004; 15(10):960–7. doi: 10.1089/hum.2004.15.960 PMID: 15585111; PubMed Central PMCID: PMCPMC4118285.

72. Himori N, Yamamoto K, Maruyama K, Ryu M, Taguchi K, Yamamoto M, et al. Critical role of Nrf2 in oxidative stress-induced retinal ganglion cell death. J Neurochem. 2013; 127(5):669–80. doi: 10.1111/jnc.12325 PMID: 23721546.

73. Moi P, Chan K, Asunis I, Cao A, Kan YW. Isolation of NF-E2-related factor 2 (Nrf2), a NF-E2-like basic leucine zipper transcriptional activator that binds to the tandem NF-E2/AP1 repeat of the beta-globin locus control region. Proc Natl Acad Sci U S A. 1994; 91(21):9926–30. PMID: 7937919; PubMed Central PMCID: PMCPMC44930.

74. Zhou T, Zong R, Zhang Z, Zhu C, Pan F, Xiao X, et al. SERPINA3K protects against oxidative stress via modulating ROS generation/degradation and KEAP1-NRF2 pathway in the corneal epithelium. Invest Ophthalmol Vis Sci. 2012; 53(8):5033–43. doi: 10.1167/iovs.12-9729 PMID: 22736614.

75. Siegel D, Gustafson DL, Dehn DL, Han JY, Boonchoong P, Berliner LJ, et al. NAD(P)H:quinone oxidoreductase 1: role as a superoxide scavenger. Mol Pharmacol. 2004; 65(5):1238–47. doi: 10.1124/mol.65.5.1238 PMID: 15102952.

76. Dinkova-Kostova AT, Talalay P. NAD(P)H:quinone acceptor oxidoreductase 1 (NQO1), a multifunctional antioxidant enzyme and exceptionally versatile cytoprotector. Arch Biochem Biophys. 2010; 501 (1):116–23. doi: 10.1016/j.abb.2010.03.019 PMID: 20361926; PubMed Central PMCID: PMCPMC2930038.

77. Nayak MS, Kita M, Marmor MF. Protection of rabbit retina from ischemic injury by superoxide dismutase and catalase. Invest Ophthalmol Vis Sci. 1993; 34(6):2018–22. PMID: 8491552.

78. Chen B, Tang L. Protective effects of catalase on retinal ischemia/reperfusion injury in rats. Exp Eye Res. 2011; 93(5):599–606. doi: 10.1016/j.exer.2011.07.007 PMID: 21824472.

79. Wang B, Liu H, Yue L, Li X, Zhao L, Yang X, et al. Neuroprotective effects of pterostilbene against oxidative stress injury: involvement of nuclear factor erythroid 2-related factor 2 pathway. Brain Res. 2016. doi: 10.1016/j.brainres.2016.04.048 PMID: 27107941.

80. Jacobs-Helber SM, Wickrema A, Birrer MJ, Sawyer ST. AP1 regulation of proliferation and initiation of apoptosis in erythropoietin-dependent erythroid cells. Mol Cell Biol. 1998; 18(7):3699–707. PMID: 9632752; PubMed Central PMCID: PMCPMC108952.

81. Sevilla L, Zaldumbide A, Pognonec P, Boulukos KE. Transcriptional regulation of the bcl-x gene encoding the anti-apoptotic Bcl-xL protein by Ets, Rel/NFkappaB, STAT and AP1 transcription factor families. Histol Histopathol. 2001; 16(2):595–601. PMID: 11332715.

82. Gu D, Beltran WA, Li Z, Acland GM, Aguirre GD. Clinical light exposure, photoreceptor degeneration, and AP-1 activation: a cell death or cell survival signal in the rhodopsin mutant retina? Invest Ophthalmol Vis Sci. 2007; 48(11):4907–18. doi: 10.1167/iovs.07-0428 PMID: 17962438; PubMed Central PMCID: PMCPMC2377016.

83. Annis MG, Yethon JA, Leber B, Andrews DW. There is more to life and death than mitochondria: Bcl-2 proteins at the endoplasmic reticulum. Biochim Biophys Acta. 2004; 1644(2–3):115–23. doi: 10.1016/j.bbamcr.2003.07.001 PMID: 14996496.

84. Distelhorst CW, Shore GC. Bcl-2 and calcium: controversy beneath the surface. Oncogene. 2004; 23 (16):2875–80. doi: 10.1038/sj.onc.1207519 PMID: 15077150.

85. Jang JH, Surh YJ. Potentiation of cellular antioxidant capacity by Bcl-2: implications for its antiapoptotic function. Biochem Pharmacol. 2003; 66(8):1371–9. PMID: 14555211.